Gas Hydrate Inhibition: A Review of the Role of Ionic Liquids

ARTICLE *in* INDUSTRIAL & ENGINEERING CHEMISTRY RESEARCH · OCTOBER 2014

Impact Factor: 2.59 · DOI: 10.1021/ie503559k

6 AUTHORS, INCLUDING:

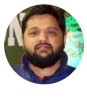

Tariq Mohammad

Qatar University

51 PUBLICATIONS **567** CITATIONS

SEE PROFILE

Santiago Aparicio

Universidad de Burgos

120 PUBLICATIONS **1,479** CITATIONS

SEE PROFILE

Mert Atilhan

Qatar University

101 PUBLICATIONS **962** CITATIONS

SEE PROFILE

Majeda A.M Khraisheh

Qatar University

79 PUBLICATIONS **2,710** CITATIONS

SEE PROFILE

I&EC research
Industrial & Engineering Chemistry Research

Review

pubs.acs.org/IECR

Gas Hydrate Inhibition: A Review of the Role of Ionic Liquids

Mohammad Tariq,[†] David Rooney,[‡] Enas Othman,[§] Santiago Aparicio,[▽] Mert Atilhan,*[,†] and Majeda Khraisheh*[,†]

[†]Department of Chemical Engineering, College of Engineering, Qatar University, P.O. Box 2713, Doha, Qatar

[‡]School of Chemistry and Chemical Engineering, Queen's University Belfast, Belfast, UKBT9 5AG, Northern Ireland

[§]Chemical Engineering Department, Texas A&M University, Doha, Qatar

[▽]Department of Chemistry, University of Burgos, Burgos, Spain

Supporting Information

ABSTRACT: Ionic liquids (ILs) are popular designer green chemicals with great potential for use in diverse energy-related applications. Apart from the well-known low vapor pressure, the physical properties of ILs, such as hydrogen-bond-forming capacity, physical state, shape, and size, can be fine-tuned for specific applications. Natural gas hydrates are easily formed in gas pipelines and pose potential problems to the oil and natural gas industry, particularly during deep-sea exploration and production. This review summarizes the recent advances in IL research as dual-function gas hydrate inhibitors. Almost all of the available thermodynamic and kinetic inhibition data in the presence of ILs have been systematically reviewed to evaluate the efficiency of ILs in gas hydrate inhibition, compared to other conventional thermodynamic and kinetic gas hydrate inhibitors. The principles of natural gas hydrate formation, types of gas hydrates and their inhibitors, apparatuses and methods used, reported experimental data, and theoretical methods are thoroughly and critically discussed. The studies in this field will facilitate the design of advanced ILs for energy savings through the development of efficient low-dosage gas hydrate inhibitors.

1. INTRODUCTION

Gas hydrates are crystalline solids in which gas molecules are trapped inside the three-dimensional (3-D) cages of hydrogen-bonded water molecules. Gas hydrates are formed only in the presence of appropriately sized guest molecules. The most popular molecules that form gas hydrates are methane (CH_4), ethane (CH_3CH_3), propane ($CH_3CH_2CH_3$), and CO_2. Hydrates are generally stable under high-pressure and low-temperature conditions.[1−4]

Although gas hydrates are chemically interesting compounds, they are industrially problematic. In particular, natural gas hydrates cause problems not only during the construction stage but also during the operational stages of process facilities such as platforms, pipelines, and other engineering structures.[5−7] Gas hydrates are easily formed in pipelines, producing gas wells before the gas is dehydrated. Prevention of gas hydrate formation elicits substantial investment, amounting to 10%−15% of the production cost.[8]

Hydrates are formed by the slow cooling of a fluid in a pipeline or by the rapid cooling caused by depressurization across valves or through turbo expanders. Studies have shown that gas hydrates in pipelines and petrochemical processes are formed under four conditions: (i) coexistence of water, (ii) natural gas components, (iii) low temperatures, and (iv) high pressures. Other factors favoring gas hydrate formation include high fluid velocity, agitation, pressure, pulsation (or any source of fluid turbulence), and the presence of CO_2 and H_2S.[9]

Gas hydrates consist of hydrogen-bonded water molecules with cavities inhabited by guest molecules under certain operating temperature and pressure conditions.[10−12] Because gas hydrates always comprise >85 mol % water, their properties are considered to be variations of those of ice.[13] For example, gas hydrates exhibit 20-fold higher mechanical strength than does ice.[14,15]

There are three main crystallographic structures for gas hydrates—cubic structure I (sI), cubic structure II (sII), and hexagonal structure H (sH)—which differ in cavity size and shape (see Figure 1).The type of gas hydrate structure formed

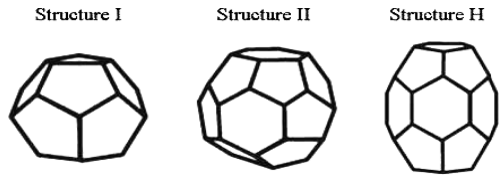

Figure 1. Types of gas hydrate crystal structures: cubic structure I (sI), cubic structure II (sII), and hexagonal structure H (sH).

is mainly determined by the size of the guest gas molecules trapped in the cavities.[4,16−20] For example, cubic structure I consists of small hydrate lattices that can only contain small gas molecules such as CH_4. Cubic structure II is larger, more complex, and capable of accommodating large hydrocarbon molecules, whereas hexagonal structure H is capable of accommodating much larger molecules, such as isopentane, which is a branched chain hydrocarbon.

From both economic and operational safety perspectives, it is essential to understand the formation kinetics of gas hydrates,

Received: July 17, 2014
Revised: October 22, 2014
Accepted: October 23, 2014

   dx.doi.org/10.1021/ie503559k | Ind. Eng. Chem. Res. XXXX, XXX, XXX−XXX

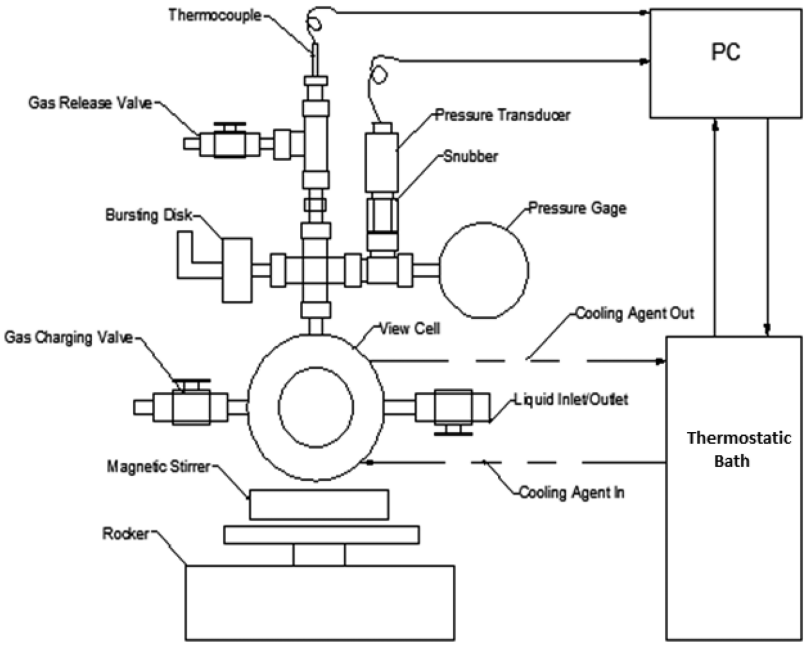

Figure 2. Schematic diagram of a typical experimental setup for studying gas hydrate dissociation conditions.

i.e., where and when natural gas hydrates are formed, for better management and control of this phenomenon.[21−24] Several studies during the past decade have indicated that understanding the formation mechanism of natural gas hydrates may help in devising alternative methods for natural gas transportation,[25−28] but no single clear mechanism has been established yet. Currently, four techniques are used to mitigate the gas hydrate formation: (i) system heating, (ii) depressurization, (iii) water removal, and (iv) inhibition.[6,29] Under many circumstances, the use of inhibitors for gas hydrate inhibition is the only feasible choice.

Currently, mainly three types of inhibitors are used: thermodynamic inhibitors, kinetic inhibitors, and antiagglomerate gas hydrate inhibitors. Thermodynamic inhibitors shift the equilibrium hydrate dissociation/stability curve, i.e., the hydrate−aqueous liquid−vapor equilibrium (HLVE) curve, to lower temperatures and high pressures, thus avoiding gas hydrate formation.[30] Generally, these compounds (inhibitors) form hydrogen bonds with water molecules, thus preventing the formation of ordered cages for holding gas molecules. Thermodynamic inhibitors are used at high concentrations, up to 50 wt %.[31] Because oil and natural gas exploration and production has now moved to deeper seas, the addition of such an inhibitor can be expensive and environmentally prohibitive. Kinetic gas hydrate inhibitors do not prevent the formation of gas hydrates; rather, they hinder the process by slowing down the hydrate nucleation and/or growth process. These materials interfere with the growth of hydrate crystals for a longer period than the residence time of water in the pipeline. Kinetic gas hydrate inhibitors are effective at a low dosage (<1 wt %) and are thus expected to have economic and environmental advantages.[2,32−34] Thermodynamic inhibitors bind free water molecules by hydrogen bonding to prevent the formation of gas hydrates, and, hence, they are needed in large quantities. On the other hand, kinetic gas hydrate inhibitors prevent crystal nucleation, and, hence, they are needed in small quantities. Another reason for the required lower amount may be the size (molar volume) of the molecule used. A combination of thermodynamic and kinetic gas hydrate inhibitors is required to provide better results.[26] Antiagglomerates do not prevent the formation of gas hydrate particles; however, they inhibit the agglomeration of these particles to form bigger clusters. Thus, the gas hydrate particles remain dispersed in the hydrocarbon phase and cannot plug the pipeline. A combination of antiagglomerates and kinetics inhibitors is also known as low-dosage hydrate inhibitors (LDHIs).[35,36]

According to previous studies,[37,38] materials with strong electrostatic charges or hydrogen-bond-forming capacity can generally inhibit the formation of gas hydrates. For example, NaCl has strong electrostatic charges; methanol, poly(ethylene oxide) (PEO), and poly(*N*-vinylpyrrolidone) (PVP) form strong hydrogen bonds with water.[39−41] Based on this concept, more effective gas hydrate inhibitors need to be discovered.

Ionic liquids (ILs) have been developed as both designer solvents and green chemicals, because their structure and physical properties can be fine-tuned for a specific application.[42,43] The ability to design ILs with specific functionalities is one of the greatest attractions, particularly when combined with other well-known properties, such as significantly low vapor pressure, compared to the molecular counterparts.[44−46] Although this research area is still in its initial stage, sufficient data is available on the first-generation ILs for their potential to act as dual-functional, thermodynamic and kinetic, gas hydrate inhibitors. In this review, we will systematically summarize the published data on this subject in the literature to date,[47−65] so that important conclusions can be drawn, which would work as a guide to further develop this potentially interesting and important area of research.

Another objective of this review is to attract the attention of the IL research community to design and test new LDHIs based on ILs that are easy to synthesize, biodegradable, nontoxic, noncorrosive, recyclable, and economically feasible. Any breakthrough in this direction will significantly contribute to the emerging field of IL science and the oil and natural gas industry.

dx.doi.org/10.1021/ie503559k | *Ind. Eng. Chem. Res.* XXXX, XXX, XXX−XXX

2. EXPERIMENTAL APPARATUSES AND METHODS

A survey of the literature indicates that most of the commonly used methods to study the thermodynamics and kinetics of gas hydrate inhibition have been applied to study the effect of ILs on gas hydrate formation. Researchers generally used the techniques readily available at their laboratories, and, in only rare cases, the experimental results have been obtained using different methods for the same sample. The most commonly used methods for studying the thermodynamics and kinetics of gas hydrate formation in the presence of ILs included high-pressure cells,[51,53,55,57,56,60] crystallizers,[52] reactors,[61−63] and differential scanning calorimetry (DSC).[48,49,59] The choice of these methods does not necessarily indicate their superiority over others, but rather reflects their availability.

In this section, we will describe briefly the experimental setup and methods used in different laboratories to study the gas hydrate inhibition by ILs. We will divide this section into two parts: one for the methods and apparatuses used to study the thermodynamic gas hydrate inhibition by ILs and another for the methods used to study the kinetic inhibition by ILs. Some research groups used the same setup but different methods to study both the aspects of gas hydrate inhibition by ILs.[48,49]

2.1. Experimental Setups Used To Study the Thermodynamics of Gas Hydrate Inhibition. The typical components of an apparatus to study the thermodynamics of gas hydrates are schematically shown in Figure 2. The apparatus generally contains a vessel (cell) of a specific volume that can withstand high pressures, a magnetic stirrer (turbulence is an essential requirement for gas hydrate formation, as mentioned earlier in the Introduction), and with/without window(s)/camera to visually observe the phenomena. High-precision temperature and pressure probes and gauge/transducer, respectively, are required for the detection of the change in these parameters to confirm the formation of gas hydrates. Sometimes, a data acquiring software is used to register the data.

The apparatuses used by various research groups to study the IL gas hydrate inhibition abilities are listed in Table 1. Clearly, the assemblies of the apparatuses are almost similar; the only differences observed are in the volume and pressure-withstanding capacity of the vessels.

2.1.1. Methods Used To Obtain Thermodynamic (HLVE) Data. Most of the research groups used the isochoric pressure-search method[66−68] to obtain the HLVE data for the gas hydrates in the absence/presence of ILs. In this method, the vessel is charged with a solution with/without the inhibitor and gas. After the temperature and pressure of the system reach constant values, where gas hydrates cannot form, the temperature is lowered slowly to form the gas hydrates. The formation of gas hydrates in the vessel can be detected by a pressure drop in the vessel and/or confirmed by visual observation when the cell is equipped with sight windows or a boroscope. The temperature then is increased in very small steps of ∼0.1 K h^{-1}. The interval time of each step should be sufficient enough (24 h) to achieve a steady-state equilibrium at each temperature. A pressure−temperature ($P-T$) diagram is obtained (Figure 3) for each experimental run from which the equilibrium point can be obtained. The point at which the $P-T$ curve sharply changes is considered to be the equilibrium point.

2.2. Experimental Setups Used To Study the Kinetics of Gas Hydrate Inhibition. Similar apparatuses used to study the thermodynamics of gas hydrate formation were used for the kinetic studies. However, the objective of the experiment was to evaluate the rate of crystal growth. A brief summary of the setups used for this purpose is shown in Table 2.

2.2.1. Methods Used To Obtain Kinetics (Induction Time for Gas Hydrates) Data. Measurement of the induction time for each sample is repeated many times. The variations in the measured induction times can be attributed to a natural phenomenon (crystallization is a complex phenomenon), which is dependent on the number of repeated experiments. In a typical experiment, the sample solutions for gas hydrate formation were heated to a certain temperature and maintained

Table 1. Apparatuses Used To Study the Thermodynamics of Gas Hydrate Formation/Dissociation in the Presence of ILs[a]

group	vessel	volume (cm^3)	pressure (MPa)
Peng et al.[51]	cylindrical high-pressure cell with 2 windows	420	20
Li et al.[52]	cylindrical hydrate crystallizer stainless steel 2 windows magnetic stirrer controllable	416	30
Tumba et al.[53]	stainless steel cylindrical cell with magnetic stirrer	60	20
Nazari et al.[54]	high-pressure apparatus (Paar Instruments)	300	NA
Kim and Kang[55,57]	high-pressure cell with magnetic stirrer	220	NA
Makino et al.[56]	high-pressure cell, sapphire window with stirrer	NA	NA
Partoon et al.[60]	Hydrval, motor-driven PVT cell, sapphire chamber, magnetic stirrer, camera attached	80	20
Zare et al.[61]	stainless steel stirrer reactor (Paar Instruments)	300	NA
Chun and Jafar[62]	high-pressure reactor including magnetic stirrer	130	NA
Keshavaraz et al.[63]	high-pressure reactor with visual detection	NA	NA
Adidharma and co-workers[48,49,59]	high-pressure SETARAM micro differential scanning calorimetry	0.5	40

[a]NA = not applicable.

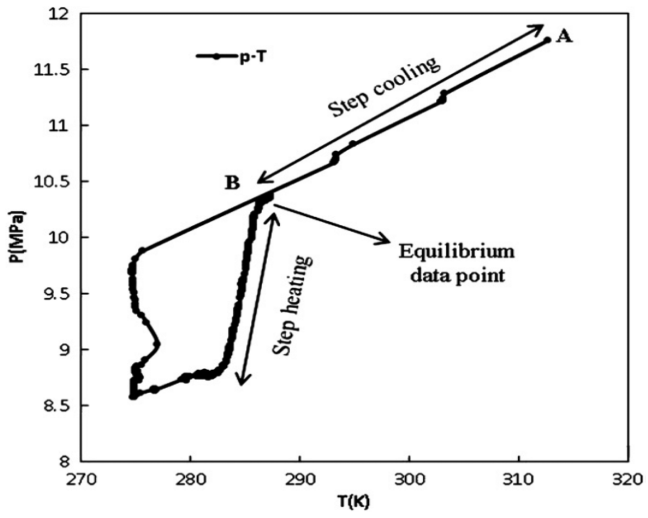

Figure 3. A typical pressure−temperature ($P-T$) diagram obtained by the isochoric pressure-search method for the CH_4 + IL + H_2O system indicating the equilibrium gas hydrate dissociation point. (Reprinted with permission from ref 61. Copyright 2013, Elsevier, Amsterdam.)

dx.doi.org/10.1021/ie503559k | Ind. Eng. Chem. Res. XXXX, XXX, XXX−XXX

Table 2. Apparatuses Used To Study the Kinetics of Gas Hydrate Formation/Dissociation in the Presence of Ionic Liquids (ILs)

group	vessel	volume (cm^3)
Del Villano and Kelland[50]	high-pressure sapphire and stainless steel autoclave	NA
Nazari et al.[54]	high-pressure thermostated stirring reactor with six glass-jacketed vessels and a multichannel magnetic stirrer	300
Kim and Kang[55,57]	high-pressure cell with a magnetic stirrer	220
Makino et al.[56]	high-pressure cell, sapphire window with stirrer	NA
Kitajima et al.[58]	high-pressure cell with magnetic stirring rod	NA

there for a few hours to minimize any memory effect. The formation of gas hydrates progressed through the well-known steps: gas dissolution, crystal nucleation, and growth. The induction times of the sample under specific conditions were determined at the end of dissolution.[69,70] The pressure of the gas and temperature of the solution were recorded under magnetic stirring. At the onset of gas hydrate formation, a sudden decrease in pressure is observed, as shown in Figure 4. The time (t_s) and pressure (P_s) at the onset of the gas hydrate formation were recorded. The time taken from the beginning to t_s is the "induction time for gas hydrates".

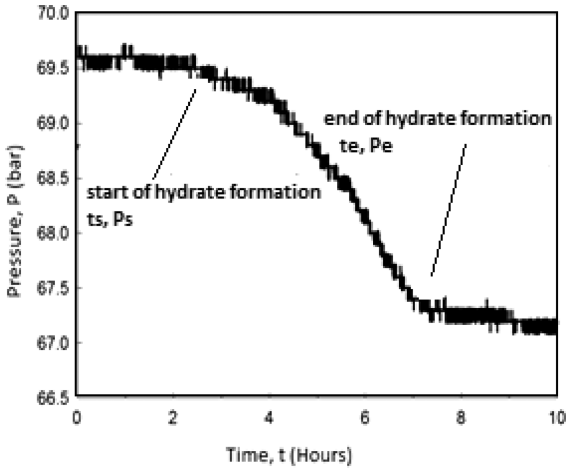

Figure 4. Typical $P-T$ diagram used to measure the induction time for gas hydrates, as adapted from ref 55.

2.3. Differential Scanning Calorimetry (DSC) Analysis for Kinetics and Thermodynamics of Gas Hydrates. Adidharma and co-workers[48,49,59] used the SETARAM high-pressure micro-DSC (HP-DSC) system to obtain the dissociation temperature and induction time for the formation of CH_4 hydrates. The apparatus can operate up to a pressure of 400 bar, with an accuracy of ±1 psi and in the temperature range from −45 °C to 120 °C. Two gas-tight high-pressure vessels were used for the measurements: one was used as the reference and other contained the sample solution and was made of Hastelloy C276 and had a volume of 0.5 mL. Two experimental modes were used: isothermal and nonisothermal modes. In the nonisothermal mode, where the onset temperature for the dissociation of CH_4 hydrates with/without inhibitors in the pressure range of 30−110 bar was studied. The thermal cycle contains two steps: a cooling step (from 25 °C to −20/−25 °C) and a heating step, in which the system returned to room temperature at a slow heating rate of 0.3 °C min^{-1}. In the isothermal mode, the induction time for gas hydrates with/without inhibitors at −12 °C and 114 bar was studied. The thermal cycle in this mode contains three steps: (1) a cooling step, where the system temperature decreased from 25 to −12 °C at a rate of 5 °C min^{-1}; (2) an isothermal step, at −12 °C, where the induction time for gas hydrates was measured; and (3) a heating step, where the system temperature increased from −12 °C to 25 °C. The induction time for gas hydrates in the DSC measurements is the time elapsed in the isothermal step when the gas hydrates were first detected.

It should be emphasized here that one of the basic issues in selecting a reliable technique for obtaining good-quality data is the accuracy and uncertainty of the measurement technique. The important variables for current study are the uncertainties in composition of the sample, the temperature, the pressure, and the apparatus-specific constant (which is dependent on the type of apparatus). Surprisingly few works have reported them in detail. Some authors[51,53,56,60,61,63] have reported an uncertainty of ±0.1 K in temperature measurements, whereas others[48,49,59] have reported it have an accuracy of ±0.4 K. Uncertainties in pressure measurements are reported[51,53,56,60,61,63] in the range of ±0.01% to ±0.05% of the full scale of the pressure sensor measuring capability. The uncertainty in the reported composition[53] is on the order of ±0.01 units, and, in some other works,[59,63] the samples were prepared with an accuracy of ±0.0001 g.

As far as the advantages and disadvantages of different techniques are concerned, the high-pressure cells[51,56,60,63] or crystallizer[52] with large volumes and sapphire windows are the best option, since one can validate the formation of hydrates by observing it. However, the problem with these cells is that a large sample quantity is required, which, in the case of ILs, becomes an economic hurdle. However, the micro-DSC[48,49,59] is a good option which requires a small amount of sample; however, on the other hand, overall uncertainties due to small sample size are too high, compared to classical methods. Moreover, mixing is an issue here.

The above discussion indicates that the most reliable technique to perform the hydrate dissociation experiments will be the one where the conditions are more closely related to the realistic (pipelines) ones. Thus, when the volume is large, since it is a bulk phenomenon, mixing is optimum, so that the turbulence can help the crystallization to felicitate and the mass transfer is adequate; this would be the ideal technique. However, there are many ways to optimize these parameters, where one can choose the best option available as per the requirements.

3. DATABASE RATIONALE AND GROUPING

All the available data on ILs, as the gas hydrate inhibitors, were collected, and a database was formed (see Table 3) to systematically evaluate the effects of various factors affecting the performance of ILs for the specified task. To date, 14 articles,[47−53,57−63] 4 conference proceedings,[54−56,64] and a patent[65] are available on this subject. After the appearance of only one article on this subject in 2008, the growth has been slow but significant (given the amount of time required to produce good quality data), because 6 studies[59−64] have already been reported so far in 2013. The systems studied, the role of

dx.doi.org/10.1021/ie503559k | Ind. Eng. Chem. Res. XXXX, XXX, XXX−XXX

Table 3. List of Ionic Liquids (ILs) and the Systems Studied for Gas Hydrate Inhibition, Their Role as Kinetic Hydrate Inhibitors (KHIs), Thermodynamic Inhibitors (THIs), and the Concentrations of ILs Used

sample	ionic liquid	gas	IL tested for	conc (wt %)	reference
1	$[C_4C_1im][BF_4]$	CO_2	KHI + THI	0.0008−0.1 mol %	47
2	$[C_2C_1im][BF_4]$	CH_4	KHI + THI	0.1−10	48
3	$[C_4C_1im][BF_4]$	CH_4	KHI + THI	10	48
4	$[C_2C_1im][N(CN)_2]$	CH_4	KHI + THI	10	48
5	$[C_2C_1im][CF_3SO_3]$	CH_4	KHI + THI	10	48
6	$[C_2C_1im][C_2SO_4]$	CH_4	KHI + THI	10	48
7	$[C_2C_1im]Cl$	CH_4	KHI + THI	10	49
8	$[C_4C_1im]Cl$	CH_4	KHI + THI	10	49
9	$[C_2C_1im]Br$	CH_4	KHI + THI	10	49
10	$[C_4C_1im]Br$	CH_4	KHI + THI	10	49
11	$[C_3C_1im]I$	CH_4	KHI + THI	10	49
12	$[C_4C_1im]I$	CH_4	KHI + THI	10	49
13	$[C_2C_1im][BF_4]$	SNG	KHI	5000−10000 ppm	50
14	$[C_4C_1im][BF_4]$	SNG	KHI	10000 ppm	50
15	$[C_4C_1im]Cl$	CO_2	THI/Sep of IL		51
16	$[C_6C_1im]Cl$	CO_2	THI/Sep of IL		51
17	$[C_8C_1im]Cl$	CO_2	THI/Sep of IL		51
18	$[C_4C_1im][BF_4]$	CO_2	THI/Sep of IL		51
19	$[C_6C_1im][BF_4]$	CO_2	THI/Sep of IL		51
20	$[C_4C_1im][TFA]$	CO_2	THI/Sep of IL		51
21	$[C_4C_1im][PF_6]$	CO_2	THI/Sep of IL		51
22	$[C_1C_1im]I$	CH_4	THI	0.1 mass fraction	52
23	$[C_2C_1im]I$	CH_4	THI	0.1 mass fraction	52
24	$[OHC_2C_1im)Cl$	CH_4	THI	0.1 mass fraction	52
25	$[N_{1111}]Cl$	CH_4	THI	0.1 massfraction	52
26	$[N_{111C2OH}]Cl$	CH_4	THI	0.1 mass fraction	52
27	$[P_{4441}][C_1SO_4]$	CH_4	THI	0.2611−0.5007 mass fraction	53
28	$[P_{4441}][C_1SO_4]$	CO_2	THI	0.2611−0.5007 mass fraction	53
29	$[C_4C_1im][BF_4]$	CH_4	THI/KHI	0.6−7	54
30	$[C_4C_1im][C_1SO_4]$	CH_4	THI/KHI	0.6−7	54
31	$[OHC_2C_1Pyrr]Cl$	CH_4	THI/KHI	0.1−10	55
32	$[OHC_2C_1Pyrr][BF_4]$	CH_4	THI/KHI	0.1−10	55
33	$[C_4C_1Pyrr]Br$	CH_4	THI/KHI	0.1−10	55
34	$[C_4C_1Pyrr][BF_4]$	CH_4	THI/KHI	0.1−10	55
35	$[2\text{-}(OHC_2)C_1Mor]Br$	CH_4	THI/KHI	0.1−10	55
36	$[2\text{-}(OHC_2)C_1Mor][BF_4]$	CH_4	THI/KHI	0.1−10	55
37	$[C_2C_1im]Br$	CO_2	THI/KHI	0.10−1.04 mol %	56
38	$[C_2C_1im][NO_3]$	CO_2	THI/KHI	0.10−1.04 mol %	56
39	$[C_2C_1im][BF_4]$	CO_2	THI/KHI	0.10−1.04 mol %	56
40	$[C_2C_1im][CF_3SO_3]$	CO_2	THI/KHI	0.10−1.04 mol %	56
41	$[C_2C_1im][BF_4]$	CH_4	THI/KHI	0.1−10	57
42	$[2\text{-}(OHC_2)C_1Pyrr][BF_4]$	CH_4	THI/KHI	0.1−10	57
43	$[C_4C_1Pyrr][BF_4]$	CH_4	THI/KHI	0.1−10	57
44	$[C_4C_1im][PF_6]$	CH_4	KHI	0−1000 ppm	58
45	$[C_2C_1im]Cl$	CH_4	THI	5−40	59
46	$[C_2C_1im]Br$	CH_4	THI	20	59
47	$[C_2C_1im]Br + [C_2C_1im]Cl$ (1:1)	CH_4	THI	20	59
48	$[C_2C_1im]Cl$ + MEG (1:1)	CH_4	THI	10−30	59
49	$[C_2C_1im]Cl$ + NaCl (1:1)	CH_4	THI	10	59
50	$[C_2C_1im]Cl$	CH_4	THI	0.1−1	60
51	$[(OHC_2)C_1im]Cl$	CH_4	THI	0.1−1	60
52	$[C_4C_1im][C_1SO_4]$	CH_4	THI	10	61
53	$[C_2C_1im][HSO_4]$	CH_4	THI	10	61
54	$[C_2C_1im][C_2SO_4]$	CH_4	THI	8−10	61
55	$[C_4C_1im][BF_4]$	CH_4	THI	10	61
56	$[2\text{-}(OHC_2)C_1im][BF_4]$	CH_4	THI	10−20	61
57	$[C_2C_1im][BF_4]$	CO_2	THI/KHI	0.1−10.0	62
58	$[C_4C_1im][BF_4]$	CH_4	THI	0.10−0.20 mass fraction	63
59	$[C_4C_1im][N(CN)_2]$	CH_4	THI	0.10 mass fraction	63
60	$[N_{2222}]Cl$	CH_4	THI	0.10 mass fraction	63

dx.doi.org/10.1021/ie503559k | Ind. Eng. Chem. Res. XXXX, XXX, XXX−XXX

Table 3. continued

sample	ionic liquid	gas	IL tested for	conc (wt %)	reference
61	$[2,3\text{-}(OHC_3)_2C_1im][f_2N]^a$	CH_4	THI/KHI	0.5−1.0 mol %	64
62	$[2\text{-}(OHC_2)C_1im][f_2N]^a$	CH_4	THI/KHI	0.5−1.0 mol %	64
63	$[C_2C_1im][BF_4]^a$	CH_4	THI/KHI	0.5−1.0 mol %	64
64	$[C_4C_1im][BF_4]^a$	CH_4	THI/KHI	0.5−1.0 mol %	64
65	$[C_4C_1im][OAc]^a$	CH_4	THI/KHI	0.5−1.0 mol %	64
66	$[C_2C_1im][C_2SO_4]^a$	CH_4	THI/KHI	0.5−1.0 mol %	64

[a]Studied using molecular dynamics simulations.

ILs, and concentrations of ILs are shown in Table 3. This table shows a total of 66 systems studied in various capacities. Fifty (50) systems were reported for CH_4 hydrates, 14 systems were reported for CO_2 hydrates, and only 2 systems were reported for synthetic natural gas (SNG) hydrates. Most of the ILs studied belong to the imidazolium family and a few ILs belong to the pyrrolidinium, ammonium, phosphonium, and morpholinium families. Clearly, 1-butyl-3-methylimidazolium tetrafluoroborate ($[C_4mim][BF_4]$) is the favorite IL, as it has been studied the most (8 times).

4. ANALYSIS OF REPORTED DATA

To make the text more reader-friendly, we decided to divide the data analysis section in two parts: The first part reports the data on the effect of ILs on the HLVE curves of gas hydrates, and the second part reports the kinetic gas hydrate inhibition studies in the presence of ILs. Because most of the directly comparable data in the open literature are available for thermodynamic gas hydrate inhibition, we further divided the first group into several subgroups to evaluate the direct structural effects of ILs on the HLVE curves. The discussion will be based on the (sub)groups as summarized in Chart 1.

4.1. ILs as Thermodynamic Gas Hydrate Inhibitors. To test the effect of ILs on the thermodynamics of gas hydrate formation/dissociation conditions, the HLVE curves in the absence/presence of ILs were recorded. In this section, we will discuss the effect of the ILs used for this purpose, according to the classified groups shown in Chart 1. This will help in understanding the role of the structure and concentration of ILs in shifting the gas hydrate equilibrium in a given direction (existence of any structure−property correlations). Initially, the data on the similar systems studied by different groups will be compared, so that the discrepancies and uncertainties in the reported data will be clear. This practice is very crucial, because not only the discrepancies will be known, if there is any, in the reported values, but also wrong conclusions will be avoided based on the comparison of the reported experimental data from different sources.

Chart 1. Grouping of Ionic Liquids (ILs) Studied for CH_4 Hydrate Inhibition, as Per Their Structure[a]

Effect of Cations				Effect of Anions	
Group A		**Group C**		**Group A***	
[Cation][BF_4]		**[Cation][Br]**		**[C_2C_1im][X]**	
C_2C_1im	BF_4	C_2C_1im	Br	C_2C_1im	BF_4
C_4C_1im	BF_4	C_4C_1im	Br	C_2C_1im	Cl
2-$(OHC_2)C_1im$	BF_4	C_4C_1Pyrr	Br	C_2C_1im	Br
C_4C_1Pyrr	BF_4	2-$(OHC_2)C_1Mor$	Br	C_2C_1im	I
OHC_2C_1Pyrr	BF_4			C_2C_1im	$N(CN)_2$
2-$(OHC_2)C_1Pyrr$	BF_4	**Group D**		C_2C_1im	HSO_4
2-$(OHC_2)C_1Mor$	BF_4	**[Cation][I]**		C_2C_1im	C_2SO_4
		C_1C_1im	I	C_2C_1im	CF_3SO_3
Group B		C_2C_1im	I		
[Cation][Cl]		C_3C_1im	I	**Group B***	
C_2C_1im	Cl	C_4C_1im	I	**[C_4C_1im][X]**	
C_4C_1im	Cl			C_4C_1im	BF_4
OHC_2C_1im	Cl	**Group E**		C_4C_1im	Cl
$(OHC_2)C_1im$	Cl	**[Cation][C_1SO_4]**		C_4C_1im	Br
N_{1111}	Cl	C_4C_1im	C_1SO_4	C_4C_1im	C_1SO_4
N_{2222}	Cl	P_{4441}	C_1SO_4	C_4C_1im	$N(CN)_2$
$N_{111C2OH}$	Cl			C_4C_1im	I
OHC_2C_1Pyrr	Cl			C_4C_1im	OAc
				C_4C_1im	PF_6

[a]Groups A−E consist of those ILs, where the cation is changed and anion is fixed, whereas Groups A* and B* consist of those ILs, where the cation is fixed and anion is changed.

4.1.1. Comparison of HLVE Data from Different Sources. Figure 5 shows the HLVE data points for CH_4 hydrates reported by Zare et al.,[61] Keshavaraz et al.,[63] and Xiao and Adidharma[48] in the presence of 10 wt % $[C_4mim][BF_4]$ and from Nazari et al.[54] in the presence of 7 wt % of a similar IL.

The reference lines (solid lines) in the HLVE curve for CH_4 hydrates (in the absence/presence of inhibitor) as shown in Figures 5−7 were drawn for comparison purposes. The lines were calculated using the data from different groups and correlated it using a second-order polynomial, thus providing a satisfactory regression coefficient ($R^2 = 0.998$). The comparison plots between calculated and experimental data points have been presented in Supporting Information (Figure S1), along with the references.

It is not possible to comment critically in terms of the quality of available data in the literature at present, because, in most of the cases, the accuracy and uncertainty of reported experimental data is missing. However, whenever the data are reported,[60,61] the values seem satisfactory. Another factor contributing to this issue is the purity of used ILs. Apart from that, most of the authors calibrated the apparatus (by obtaining the HLVE curves in the absence of ILs) and compared the data with the available literature values, which is essential to form a reliable study and draw conclusions. Nevertheless, the reported values from different research groups are consistent (see Figure 5). Figure 5 clearly shows the significant effect of added IL in shifting the HLVE curve toward higher pressure values, indicating that the studied IL acts similar to a typical thermodynamic inhibitor in the system.[34,48]

4.1.2. Effect of IL Concentration. Another important aspect of thermodynamic gas hydrate inhibition is the amount of added inhibitor and its effect. To address this issue, we selected few systems that contained the same ILs in different amounts and studied their effect on CH_4 hydrate dissociation conditions. The results are summarized in Figure 6a and 6b.

Figure 6a clearly shows that 10 wt % concentration of $[C_4mim][BF_4]$ shifts the dissociation conditions of CH_4 hydrate to a lower temperature by ∼1 K, while this temperature

dx.doi.org/10.1021/ie503559k | Ind. Eng. Chem. Res. XXXX, XXX, XXX−XXX

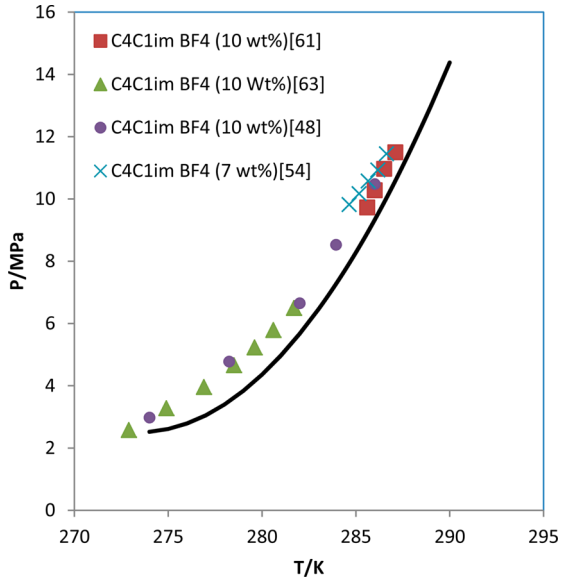

Figure 5. Comparison of the HLVE data for CH_4 hydrates in the presence of similar concentration (otherwise indicated) and the type of IL measured by different groups.[48,54,61,63] The solid black line represents the calculated HLVE data for CH_4 hydrates in the absence of any inhibitor.

is ~1.5 K when the concentration of added IL was 20 wt %.[63] Thus, the increase in the concentration of $[C_4C_1im][BF_4]$ in the aqueous solution increases the inhibition capacity of this IL for CH_4 hydrates.

Figure 6b shows similar results for $[C_2C_1im]Cl$. The increase in the concentration of IL from 0.1 wt % to 40 wt % in the aqueous solutions shifted the equilibrium toward much lower temperatures.[59,60] Thus, the thermodynamic gas hydrate inhibition effect of $[C_2C_1im]Cl$ enhanced drastically compared to $[C_4C_1im][BF_4]$ with increasing concentration of ILs in the aqueous solutions.

In both cases, the effect of IL inhibition is much lower, compared to the conventional thermodynamic inhibitor methanol in the same amount (10 wt %). However, in Figure 6b, it is noticeable that 30 wt % $[C_2C_1im]Cl$ is exhibiting a similar inhibition effect as 10 wt % methanol. The inhibition effect of these ILs on the equilibrium conditions is smaller at low pressures and becomes more significant at high pressures.

4.1.3. Effect of IL Cations (Varying Alkyl Chain Length and Substitution). To evaluate the effect of cations of ILs, the available HLVE data for CH_4 hydrates in the presence of ILs were distributed in various groups, as shown in Chart 1. Five groups were formed (A–E), where the anion is fixed in each group and the cations are changed either by varying the alkyl chain length or by adding a functional group. We plotted individual plots for each group to evaluate these effects in detail (see Figure 7).

Groups A–E can be represented as [Cation][BF_4], [Cation]-[Cl], [Cation][Br], [Cation][I], and [Cation][C_1SO_4]. The plots for the HLVE data of CH_4 hydrates in the presence of similar amount (10 wt %) of ILs added (as shown in Figure 7e for $[P_{4441}][C_1SO_4]$) in these categories are shown in Figures 7a–d.

Figures 7a–e clearly show a significant effect of the IL cations on the CH_4 hydrate dissociation conditions. The effect of alkyl chain length is clearly visible in Figures 7a–c and is more clearly visible in Figure 7d. The efficiency of ILs as

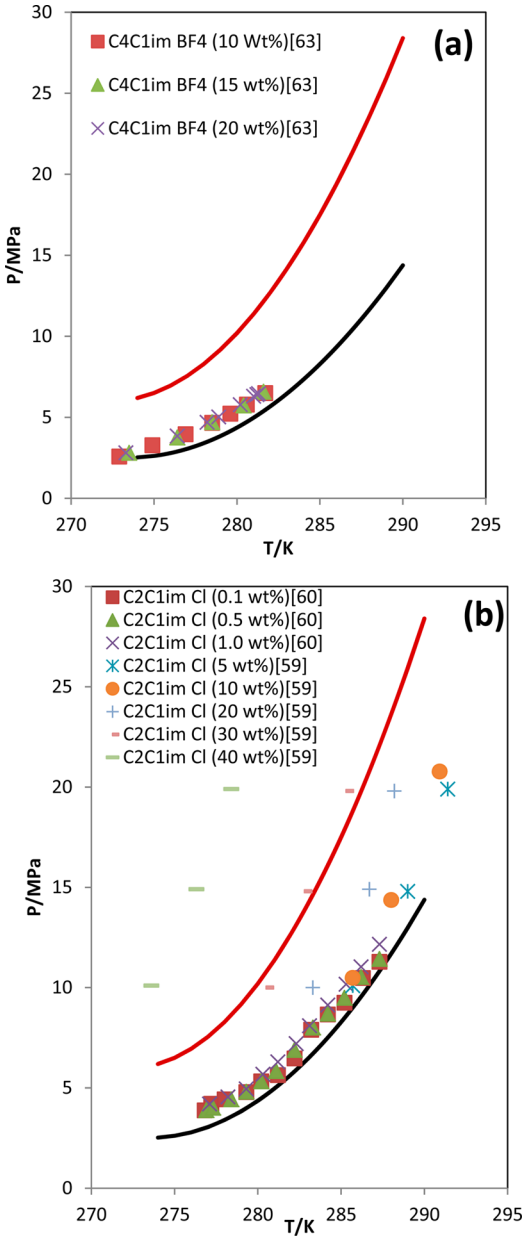

Figure 6. Effect of various concentrations of (a) $[C_4C_1im][BF_4]$ and (b) $[C_2C_1im]Cl$ on the CH_4 hydrate dissociation conditions. The solid lines represent the calculated HLVE data for CH_4 hydrates in the absence of any inhibitors (black) and in the presence of 10 wt % methanol (red).

thermodynamic gas hydrate inhibitors decreases with increasing chain length of the cation.[49,52] This is probably because of the increased hydrophobicity of ILs with the longer alkyl chain length. Moreover, the substitution of OH groups in the cation, as shown in Figures 7a and 7b, clearly enhanced the performance. This is because the IL with OH-substituted cation would be easily incorporated into the hydrogen-bonding network of water, thus making the gas hydrate formation difficult. However, this is not always the case,[52] because $[N_{1111}]$Cl showed enhanced inhibition efficiency, compared to $[N_{1112OH}]Cl$ (Figure 7b). This is probably because the hydroxylated alkyl substituent is longer in length, compared to the alkyl counterpart, thus decreasing its ability to inhibit the gas hydrate formation.[52] Moreover, Figures 7a, 7b, and 7e

dx.doi.org/10.1021/ie503559k | Ind. Eng. Chem. Res. XXXX, XXX, XXX–XXX

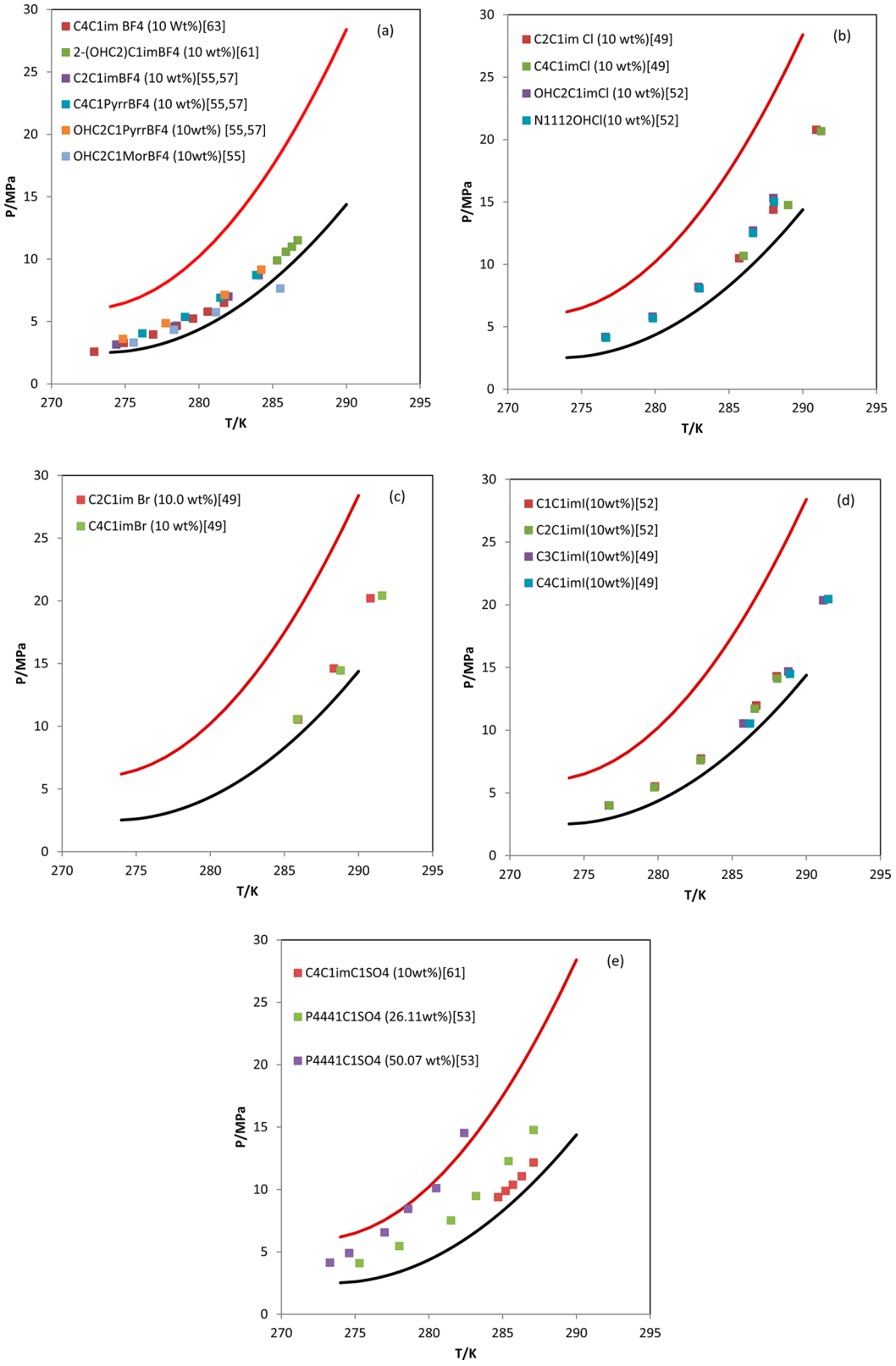

Figure 7. (a–e). Effect of cations (alkyl chain length and substitution) of 10 wt % (otherwise indicated) added ionic liquids on the HLVE curves of CH_4 hydrates. The solid lines represent the calculated HLVE data for CH_4 hydrates in the absence of any inhibitors (black) and in the presence of 10 wt % methanol (red).

clearly show that the pyrrolidinium-, ammonium-, and phosphonium-based ILs are more-effective thermodynamic inhibitors, compared to their imidazolium counterparts.[52,53,55,57]

Again, it can be inferred from the above results that none of the reported IL is performing as good as the conventional thermodynamic inhibitor, methanol, in the same concentration range. However, Figure 7e indicates that 50 wt % $[P_{4441}]$-

dx.doi.org/10.1021/ie503559k | Ind. Eng. Chem. Res. XXXX, XXX, XXX–XXX

$[C_1SO_4]$ is giving equivalent inhibition performance as 10 wt % methanol.

4.1.4. Effect of IL Anions. To investigate the effect of IL anions, the available HLVE data for CH_4 hydrate dissociation conditions in the presence of ILs with similar cations but different anions were distributed in two groups: A* and B*, as shown in Chart 2. The individual plots for each group were drawn to evaluate these effects in detail (see Figure 8).

Chart 2. Basic Structures of Cation/Anion of Ionic Liquids Used for Gas Hydrate Inhibition Studies in the Literature. Cations: (a) 1-alkyl-3-methylimidazolium $[C_nmim]$; (b) alkylpyrrolidinium $[C_nC_mPyrr]$; (c) morpholinium [Mor]; (d) tetraalkylammonium $[N_{n1,n2,n3,n4}]$; (e) tetraalkylphosphonium $[P_{n1,n2,n3,n4}]$. Anions: (f) tetrafluoroborate $[BF_4]$; (g) acetate [OAc]; (h) dicynamide $[C(CN)_2]$; (i) alkylsulfate $[C_nSO_4]$; (j) hexafluorophosphate $[PF_6]$; (k) triflate [Otf]; (l) nitrate $[NO_3]$; (m) trifluoroacetate [TFA]; (n) bis(fluorosulfonyl)imide $[f_2N]$.

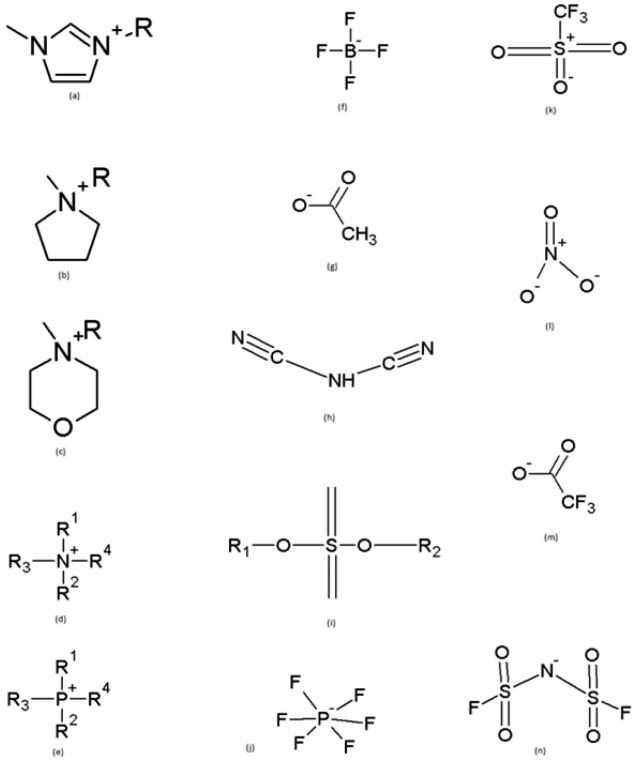

Figures 8a and 8b show that, in most of the cases, it is difficult to distinguish the individual IL data points, because most of the ILs show very similar inhibition behavior, even though it is possible to draw some conclusions from these plots. The order of the efficiency of ILs in thermodynamic CH_4 hydrate inhibition is as follows: $[C_2C_1im]Cl > [C_2C_1im]Br > [C_2C_1im]I > [C_2C_1im][BF_4] > [C_2C_1im][HSO_4] > [C_2C_1im][C_2SO_4]$ (Figure 8a) and $[C_4C_1im]Cl > [C_4C_1im]Br > [C_4C_1im]I > [C_4C_1im][C_1SO_4] > [C_4C_1im][BF_4] > [C_4C_1im][N(CN)_2]$ (Figure 8b). The thermodynamic gas hydrate inhibition efficiency for ILs with the same anion attached to shorter alkyl chain (C_2) substituent is better than that of ILs with longer alkyl chain (C_4) substituent.[51] Among all the studied ILs, $[C_2C_1im]Cl$ is the most effective IL in shifting the gas hydrate equilibrium line to lower temperatures, whereas $[C_4C_1im][N(CN)_2]$ is the least effective IL.

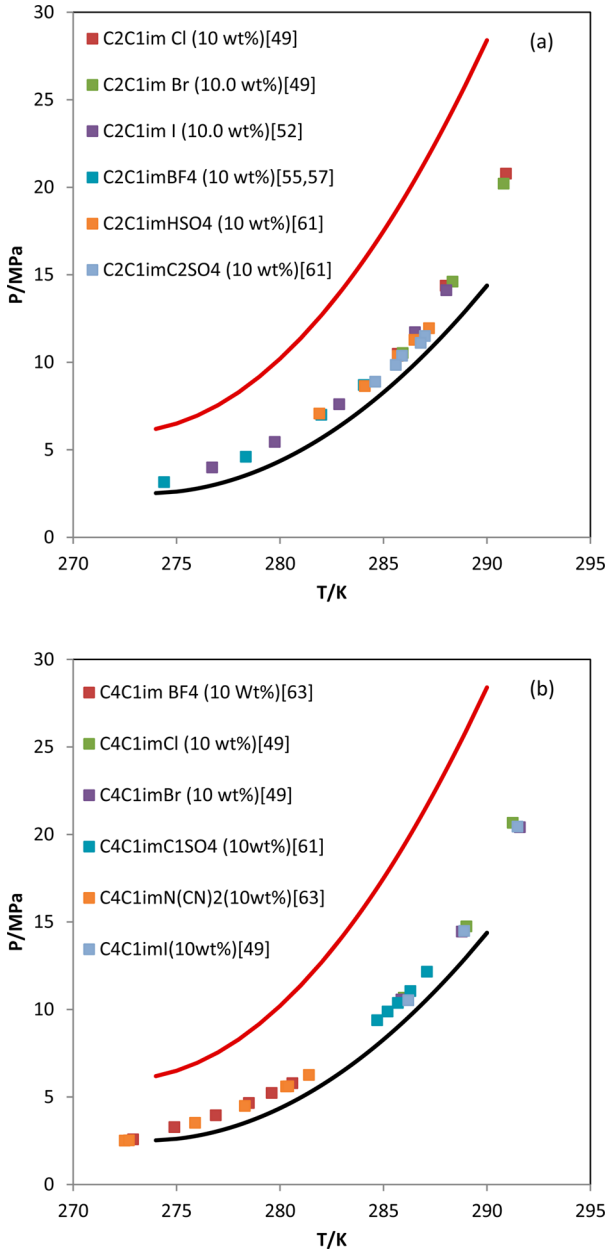

Figure 8. Effect of anions (a) $[C_2C_1im][X]$ and (b) $[C_4C_1im][X]$ of added ILs (10 wt %) on the CH_4 hydrate dissociation conditions. The solid lines represent the calculated HLVE data for the CH_4 hydrates in the absence of any inhibitors (black) and in the presence of 10 wt % methanol (red).

4.1.5. Effect of Mixtures of ILs. As shown in Table 3 (samples 47−49), three (1:1) mixtures containing ILs, $[C_2C_1im]Cl$, and $[C_2C_1im]Br$, with monoethylene glycol (MEG) and NaCl, were studied for their efficiency and possible synergistic effect in gas hydrate inhibition.[59] The system, 10 wt % $[C_2C_1im]Cl$ + MEG, exhibited a synergistic effect above a pressure of 35.2 MPa. A synergistic effect is possible for this system at higher pressures when high concentrations are used. No synergistic effect was observed for 10 wt % $[C_2C_1im]Cl$ + NaCl. For the $[C_2C_1im]Cl$ + $[C_2C_1im]Br$ system, a synergistic effect was observed above a pressure of 17.7 MPa. Pressure has a significant effect on the inhibition, depending on the type of inhibitor and concentration used. The gas hydrate inhibition efficiency of the

dx.doi.org/10.1021/ie503559k | Ind. Eng. Chem. Res. XXXX, XXX, XXX−XXX

Table 4. Studied Gas Hydrate Systems to Evaluate the Effect of Ionic Liquids (ILs) as Kinetic Gas Hydrate Inhibitors along with the Concentrations of ILs Used, Temperature, Pressure, and Induction Time (IT)

sample	IL	conc (wt %)	gas	temperature, T (°C)	pressure, P (bar)	induction time, IT (h)	reference
1	pure water		CH_4	−12	114	0.36	48
2	$[C_2C_1im][BF_4]$	10	CH_4	−12	114	6.48	48
3	$[C_4C_1im][BF_4]$	10	CH_4	−12	114	3.94	48
4	$[C_2C_1im][N(CN)_2]$	10	CH_4	−12	114	1.03	48
5	$[C_2C_1im][CF_3SO_3]$	10	CH_4	−12	114	0.4	48
6	$[C_2C_1im][C_2SO_4]$	10	CH_4	−12	114	0.56	48
7	$[C_2C_1im]Cl$	1	CH_4	−12	114	1.47	49
8	$[C_2C_1im]Br$	1	CH_4	−12	114	2.04	49
9	$[C_4C_1im]Cl$	1	CH_4	−12	114	1.85	49
10	$[C_4C_1im]Br$	1	CH_4	−12	114	2.45	49
11	$[C_4C_1im]I$	1	CH_4	−12	114	5.21	49
12	$[C_3C_1im]I$	1	CH_4	−12	114	1.29	49
13	pure water		CH_4	11	105		54
14	pure water		CH_4	11	110	1.3	54
15	pure water		CH_4	11	125	2.63	54
16	$[C_4C_1im][BF_4]$	0.6	CH_4	11	105	3.3	54
17	$[C_4C_1im][BF_4]$	0.6	CH_4	11	110	6.3	54
18	$[C_4C_1im][BF_4]$	0.6	CH_4	11	125	7.63	54
19	$[C_4C_1im][C_1SO_4]$	0.6	CH_4	11	105	0.63	54
20	$[C_4C_1im][C_1SO_4]$	0.6	CH_4	11	110	2.63	54
21	$[C_4C_1im][C_1SO_4]$	0.6	CH_4	11	125	4.3	54
22	$[C_2C_1im][BF_4]$	0.1	CH_4	1	70	0.59	55
23	$[C_2C_1im][BF_4]$	1	CH_4	1	70	1.47	55
23	$[C_2C_1im][BF_4]$	10	CH_4	1	70	1.62	55
25	$[C_4C_1Pyrr][BF_4]$	0.1	CH_4	1	70	0.40	55
26	$[C_4C_1Pyrr][BF_4]$	1	CH_4	1	70	0.97	55
27	$[C_4C_1Pyrr][BF_4]$	10	CH_4	1	70	3.89	55
28	$[OHC_2C_1Pyrr][BF_4]$	0.1	CH_4	1	70	1.03	55
29	$[OHC_2C_1Pyrr][BF_4]$	1	CH_4	1	70	1.69	55
30	$[OHC_2C_1Pyrr][BF_4]$	10	CH_4	1	70	5.71	55
31	$[2\text{-}(OHC_2)C_1Mor][BF_4]$	0.1	CH_4	1	70	0.45	55
32	$[2\text{-}(OHC_2)C_1Mor][BF_4]$	1	CH_4	1	70	1.79	55
33	$[2\text{-}(OHC_2)C_1Mor][BF_4]$	10	CH_4	1	70	6.08	55
34	pure water		CO_2	2	25	3.1	62
35	pure water		CO_2	2	30	3.5	62
36	pure water		CO_2	2	35	11.5	62
37	$[C_2C_1im][BF_4]$	0.1	CO_2	2	25	6.3	62
38	$[C_2C_1im][BF_4]$	0.5	CO_2	2	25	16.1	62
39	$[C_2C_1im][BF_4]$	1	CO_2	2	25	30.2	62
40	$[C_2C_1im][BF_4]$	0.1	CO_2	2	30	6	62
41	$[C_2C_1im][BF_4]$	0.5	CO_2	2	30	20	62
42	$[C_2C_1im][BF_4]$	1	CO_2	2	30	36.3	62
43	$[C_2C_1im][BF_4]$	10	CO_2	2	30	48	62
44	$[C_2C_1im][BF_4]$	0.1	CO_2	2	35	13.2	62
45	$[C_2C_1im][BF_4]$	0.5	CO_2	2	35	14.6	16
46	$[C_2C_1im][BF_4]$	1	CO_2	2	35	17.1	16

systems containing $[C_2C_1im]Cl$ or $[C_2C_1im]Br$ increased as the pressure increased.[59]

4.2. ILs as Kinetic Gas Hydrate Inhibitors. The effects of ILs on the rate of gas hydrate formation/crystallization have been studied. Usually, the induction time for gas hydrates, a measure of the delay in the formation of gas hydrates in the presence of an additive compared to the neat (water + gas) system, has been measured. Various methods and apparatuses have been used for this purpose. Unlike thermodynamic data, it is not possible to compare directly the induction time for gas hydrates obtained from different sources;[48] therefore, all the studied systems are listed in Table 4 and grouped in different sets, based on the method used.

The induction time for gas hydrates is an important indicator to characterize the kinetics of gas hydrate crystallization; this is the time elapsed until the onset of precipitation, which is the sum of the times for critical nucleus formation and crystal growth to a detectable size.[69,70] For heterogeneous nucleation,

dx.doi.org/10.1021/ie503559k | Ind. Eng. Chem. Res. XXXX, XXX, XXX−XXX

the nucleation rate is dependent on many factors, such as the cell wall roughness, presence of impurities and particles in the sample, and driving force. Thus, nucleation and induction time for gas hydrates are probabilistic phenomena. Because different experimental methods will obviously provide different results, to compare the performance of different gas hydrate inhibitors, the induction time for gas hydrates should be measured using the same experimental method and apparatus.[48]

Table 4 clearly shows that the CH_4 hydrate kinetic inhibition effect of 1 wt % $[C_4C_1im]I$ is comparable to that of 10 wt % $[C_2C_1im][BF_4]$. The mean value of induction time of CH_4 hydrate formation from the samples containing 1 wt % $[C_4C_1im]I$ is ~5.21 h, compared to 6.48 and 3.94 h for 10 wt % $[C_2C_1im][BF_4]$ and 10 wt % $[C_4C_1im][BF_4]$, respectively.[48,49] $[C_4C_1im]I$ was claimed to be a better kinetic gas hydrate inhibitor, with better performance even at lower concentrations, than the commercially available kinetic gas hydrate inhibitors such as Luvicap and PVcap.[49]

Nazari et al.[54] studied the kinetic inhibition effect of two ILs, namely, $[C_4C_1im][BF_4]$ and $[C_4C_1im][C_1SO_4]$ (0.6 wt %), and concluded that $[C_4C_1im][BF_4]$ is a stronger kinetic inhibitor that increased the induction time for gas hydrates by 2.8- and 4.8-fold at pressures of 105 and 110 bar, respectively, by postponing the nucleation step of CH_4 hydrate formation.

Kim et al.[55] used four ILs belonging to the imidazolium, pyrrolidinium, and morpholinium families at different concentrations (0.1−10 wt %) and studied their effect on the kinetics of CH_4 hydrate formation. The difference in the induction time among the ILs was more distinguishable at a concentration of 10 wt %. Superior inhibition effect of the ILs that contain the OH group was observed (Table 4), because this functional group facilitates the cleavage of the hydrogen bonds of water, thus delaying gas hydrate formation.

$[C_2C_1im][BF_4]$ was studied for its efficiency in delaying the CO_2 hydrate (type I) formation as a low-dosage kinetic inhibitor (0.1−1.0 wt %)[62] at a constant temperature of 275 K and varying pressures. The rate of inhibition of gas hydrate formation increased with increasing IL concentration. However, at a much higher concentration (10 wt %) and pressure (30 bar), no significant change in the induction time was observed (see Table 4).

Because of the limitations of comparing data obtained from different methods, the effect of IL cations and anions on the kinetics of gas hydrate inhibition is still not clear.

4.2.1. A Critical Work (Special Mention). Notably, Del Villano and Kelland[50] tested the kinetic gas hydrate inhibition effect of $[C_2C_1im][BF_4]$ and $[C_4C_1im][BF_4]$ under more-realistic conditions of temperature, subcooling, and reactor design, compared to those reported previously by Xiao and Adidharma.[48] The results obtained were in contrast to the observations of Xiao and Adidharma, indicating that the studied ILs provide no kinetic inhibition effect; instead, they catalyze the gas hydrate formation. Further tests revealed that the studied ILs exhibit a positive synergistic effect with commercial hydrate inhibitors. It must be stressed here that, as previously stated in the Experimental Apparatuses and Methods section, the experimental setup and method can significantly influence the results when the induction time is measured. When the conditions are more robust (more turbulence and mixing), the induction time will decrease, whereas moderate conditions provide enough relaxation time for the crystallization to occur. Chen et al.[47] studied the effect of stirring rate on the CO_2 solubility in pure water and gas hydrate nuclei formation and concluded that an optimum stirring rate should be used for such studies.

Del Villano and Kelland[50] also pointed out that the studied ILs do not degrade in seawater for 28 days, highlighting the environmental concerns about using these ILs as the alternative gas hydrate inhibitors.

5. MODELING AND COMPUTER SIMULATION ON IL−GAS HYDRATE SYSTEMS

Few reports[53,54,60,61,63,80−82] are available on the thermodynamic modeling of gas hydrates in the presence of ILs. The gas hydrate dissociation conditions are generally estimated using the model based on the equality of chemical potential of water in the aqueous phase to that in the gas hydrate phase.[71−73] For the determination of the fugacity of gas hydrate promoters/inhibitors in the gas phase, the equation of state (EOS)[74] has been applied, while the solid theory of van der Waals and Platteeuw (vdW-P)[75] has been used to estimate the fugacity of water in the gas hydrate phase. To determine the water activity in aqueous solutions that contain ILs, the nonrandom two-liquid (NRTL) activity model has been implemented.[63,76,77]

Few thermodynamic models are available for the prediction of gas hydrate equilibrium conditions in the presence of electrolyte solutions. These models are based on the effect of additives on water activity. Partoon et al.[60] used the Maddox et al.[78] model for nonelectrolyte inhibitors to evaluate the effect of ILs on CH_4 hydrate formation phase boundary. The activity of aqueous solutions was predicted using the equations of Pitzer and Mayorga.[79]

Jiang and Adhidharma[81,82] have developed the only available predictive model based on statistical associating fluid theory (SAFT) coupled with the van der Waals and Platteeuw model for hydrate phase to describe the thermodynamic properties and hydrate dissociating conditions in the presence of mixed electrolytes[81,82] and aqueous imidazolium-based IL solutions.[82] The model was validated for the effect of pressure, anion, cation alkyl chain length, and IL concentration on the hydrate inhibition.

Notably, most of these models are based on the assumption that the investigated ILs are not encapsulated in the gas hydrate cages. However, this fact requires rigorous confirmation using suitable techniques such as Raman spectroscopy, nuclear magnetic resonance (NMR), and X-ray diffraction (XRD).[53,63] On the other hand, this assumption clearly is not true for the systems including semiclathrate hydrates, e.g., in the gas hydrate former + tetrabutylammonium bromide (TBAB), tetrabutylammonium chloride (TBAC), and tetrabutylammonium fluoride (TBAF) aqueous solution systems, because the halide ions are known to participate in the structure of water cages with different structures than in the traditional clathrate hydrates.[83−88]

Only one molecular dynamics (MD) simulation study[64] has been reported on the thermodynamics and kinetics of gas hydrate inhibition in the presence of ILs. Nasrollah et al.[64] studied the thermokinetic inhibition mechanism of six imidazolium-based ILs on CH_4 clathrate hydrate formation and its growth using classical MD simulations. The ILs investigated include 1-(2,3-dihydroxypropyl)-3-methylimidazolium bis(fluorosulfonyl)imide ($[C_3(OH)_2mim][f_2N]$), 1-(2-hydroxyethyl)-3-methylimidazolium bis(fluorosulfonyl)imide ($[C_2OHmim][f_2N]$), 1-ethyl-3-methylimidazolium tetrafluoroborate ($[C_2mim][BF_4]$), $[C_4mim][BF_4]$, 1-butyl-3-methylimidazolium acetate ($[C_4mim][OAc]$), and 1-ethyl-3-methylimi-

dx.doi.org/10.1021/ie503559k | Ind. Eng. Chem. Res. XXXX, XXX, XXX−XXX

dazolium ethylsulfate ($[C_2mim][EtSO_4]$). The simulations showed that $[C_2OHmim][f_2N]$ and $[C_3(OH)_2mim][f_2N]$ are strongly hydrated, compared to other ILs, because of the hydrogen bonding between the OH groups of the cation and water molecules. They also exhibited high diffusion rates toward crystal surface and bonded to it by strong intermolecular interactions. Therefore, these two ILs are stronger thermokinetic gas hydrate inhibitors for the formation and growth of CH_4 hydrates, compared to the other ILs studied in this review, as well as conventional inhibitors such as methanol and NaCl. The simulations also revealed that the cations of $[C_3(OH)_2mim][f_2N]$ and $[C_2OHmim][f_2N]$ hinders the adsorption of water and guest molecules on the gas hydrate surface, thus inhibiting the growth of gas hydrate crystals. Moreover, $[C_3(OH)_2mim][f_2N]$ and $[C_2OHmim][f_2N]$ more probably inhibit gas hydrate formation. The results are consistent with the experimental results discussed in the previous sections, where the presence of additional OH groups enhanced the performance of a given IL as a gas hydrate inhibitor.[52,55,57,61]

6. CONCLUDING REMARKS AND PERSPECTIVES

ILs are promising materials for the future in various energy applications. The currently available data on ionic liquids (ILs) led to some important conclusions on the structure−activity relationship of ILs for gas hydrate inhibition:

(i) The more the concentration of ILs added to the system, the more effective is the shift of the equilibrium toward lower temperatures, thus leading to efficient thermodynamic inhibition.

(ii) The longer the alkyl chain of the cation of ILs, the less effective they are as inhibitors.

(iii) The presence of suitable hydrogen-bond-forming functional groups (e.g., OH, NH_2, NHCO, SO_3H) in an IL structure would provide more-efficient gas hydrate inhibitors, compared to unsubstituted ILs.

(iv) In the absence of data for a gradual change in the anions of ILs, any correlation is difficult to make.

(v) ILs can also act effectively as kinetic inhibitors; however, further studies are needed to understand the effects of different types of cations and anions of ILs on the kinetics of gas hydrate formation.

(vi) Mixtures of ILs and IL + conventional hydrate inhibitors exhibit synergism and promising results in their efficiency; thus, more combinations should be explored.

(vii) Although thermodynamic models are available in the literature, most of them assume that ILs are excluded from the clathrate hydrate (gas hydrate) cages.

Since most of the ILs tested toward their efficiency as hydrate inhibitors belongs to imidazolium family or having fluorinated anions that are known to be toxic,[89] the composition needed to obtain the desired results also is much higher, compared to conventional inhibitors; one of the most important directions for future research in this area would be to design such ILs that are economic, biocompatible, noncorrosive, and can be used as low-dosage and dual-functional gas hydrate inhibitors.

Another important direction for future research will be to characterize the structures of gas hydrates formed in the presence of various ILs, which can lead to the development of better thermodynamic models. To this end, extensive theoretical studies using density functional theory (DFT) and other molecular dynamics (MD) calculations are required to better understand the complex phenomena of gas hydrate formation in the presence of complex ILs and other functional materials for this application.

■ ASSOCIATED CONTENT

Supporting Information

A figure showing the comparison between calculated and experimental data points for the pressure−temperature ($P-T$) line for HLVE curves, and additional references, are provided as Supporting Information. This material is available free of charge via the Internet at http://pubs.acs.org.

■ AUTHOR INFORMATION

Corresponding Authors

*E-mail: mert.atilhan@qu.edu.qa (M. Atilhan).
*E-mail: m.khraisheh@qu.edu.qa (M. Khraisheh).

Notes

The authors declare no competing financial interest.

■ ACKNOWLEDGMENTS

This work was made possible by NPRP Grant No. [05-590-2-238] from the Qatar National Research Fund (a member of Qatar Foundation). The authors would like to thank Dr. Hertanto Adidharm (USA) and Dr. Ki-Sub Kim (Korea) for providing useful thermodynamic data.

■ REFERENCES

(1) Sloan, E. D., Jr. Fundamental principles and applications of natural gas hydrates. *Nature* **2003**, *426*, 353−359.
(2) Koh, C. A. Towards a fundamental understanding of natural gas hydrates. *Chem. Soc. Rev.* **2002**, *31*, 157−167.
(3) Sloan, E. D. *Clathrate Hydrates of Natural Gases*; Marcel Dekker: New York, 1998.
(4) Sloan, E. D.; Koh, C. A. *Clathrate Hydrates of Natural Gases*, Third Edition; CRC Press: Boca Raton, FL, 2007.
(5) Atilhan, M.; Aparicio, S.; Benyahia, F.; Deniz, E. Natural Gas Hydrates. In *Advances in Natural Gas Technology*; Intech Europe: Rijeka, Croatia, 2012; Chapter 7 (DOI: 10.5772/38301).
(6) Mokhatab, S.; Wilkens, R. J.; Leontaritis, K. J. A review of strategies for solving gas-hydrate problems in subsea pipelines. *Energy Sources, Part A* **2007**, *29*, 39−45.
(7) Austvik, T.; Li, X.; Gjersten, L. H. Hydrates plug properties: Formation and removal of plugs. *Ann. N.Y. Acad. Sci.* **2000**, *912*, 294−303.
(8) Makogan, Y. F. *Hydrates of Hydrocarbons*; Penn Well Publishing Company: Tulsa, OK, 1997.
(9) Carroll, J. J. Problem is the result of industry's move to use higher pressures. *Pipeline Gas J.* **2003**, *230*, 60−61.
(10) Katz, D. L. Overview of phase behavior in oil and gas production. *J. Pet. Technol.* **1983**, *35*, 1205−1214.
(11) Katz, D. L.; Lee, R. L. *Natural Gas Engineering*; McGraw−Hill: New York, 1990.
(12) Lee, S.; Zhang, J. S.; Mehta, R.; Woo, T. K.; Lee, J. W. Methane hydrate equilibrium and formation kinetics in the presence of an anionic surfactant. *J. Phys. Chem. C* **2007**, *111*, 4734−4739.
(13) Bai, Y.; Bai, Q. *Subsea Pipelines and Risers*; Elsevier Science, Ltd.: Amsterdam, 2005.
(14) Durham, W. B.; Kirby, S. H. Peculiarities of methane clathrate hydrate formation and rheology, and the associated superheating of water ice. *Science* **1996**, *273*, 1843−1848.
(15) Durham, W. B.; Stern, L. A.; Kirby, S. H. Ductile flow of methane hydrate. *Can. J. Phys.* **2003**, *81*, 373−380.
(16) McMullan, R. K.; Mak, T. C. W.; Jeffrey, G. A. Polyhedral clathrate hydrates. XI. Structure of tetramethylammonium hydroxide pentahydrate. *J. Chem. Phys.* **1966**, *44*, 2338−2345.
(17) Mak, T. C. W. Hexamethylenetetramine hexahydrate: A new type of clathrate hydrate. *J. Chem. Phys.* **1965**, *43*, 2799−2805.

(18) Davidson, D. W.; Desando, M. A.; Gough, S. R.; Handa, Y. P.; Ratcliffe, C. I.; Ripmeester, J. A.; Tse, J. S. A clathrate hydrate of carbon monoxide. *Nature* **1987**, *328*, 418−419.
(19) Davidson, D. W.; Gough, S. R.; Handa, Y. P.; Ratcliffe, C. I.; Ripmeester, J. A.; Tse, J. S. Some structural studies of clathrate hydrates. *J. Phys., Colloq.* **1987**, 537−542.
(20) Jeffery, G. A. In *Inclusion Compounds*; Atwood, J. L., Davies, J. E. D., MacNicol, D. D., Eds.; Academic Press: London, 1984.
(21) Guo, D. B.; Song, D. S.; Chacko, J.; Ghalambor, D. A. *Offshore Pipelines*; Gulf Professional Publishing: Houston, TX, 2005.
(22) Guo, B.; Bretz, R. E.; Lee, R. L. (New Mexico Tech Research Foundations). *Method and apparatus for generating, transporting and dissociating gas hydrates*. U.S. Patent 5,473,904, Dec. 12, 1995.
(23) Sloan, E. D.; Fleyfel, F. Hydrate dissociation enthalpy and guest size. *Fluid Phase Equilib.* **1992**, *76*, 123−140.
(24) Robinson, D. B. The interface between theory and experiment. *Fluid Phase Equilib.* **1989**, *52*, 1−14.
(25) Kuznetsova, T.; Sapronova, A.; Kvamme, B.; Johannsen, K.; Haug, J. Impact of low-dosage inhibitors on clathrate hydrate stability. *Macromol. Symp.* **2010**, *287*, 168−176.
(26) Kelland, M. A. History and development of low dosage hydrate inhibitors. *Energy Fuels* **2006**, *20*, 825−847.
(27) Shin, K.; Park, Y.; Cha, M.; Huh, D.-G.; Lee, J.; Kim, S.-J.; Lee, H. Swapping phenomena occurring in deep-sea gas hydrates. *Energy Fuels* **2008**, *22*, 3160−3163.
(28) Lee, H.; Lee, J.-W.; Kim, D.-Y.; Park, J.; Seo, Y.-T.; Zeng, H.; Moudrakovski, I. L.; Retcliffe, C. I.; Ripmeester, J. A. Tuning clathrate hydrates for hydrogen storage. *Nature* **2005**, *434*, 743−746.
(29) Makogon, Y. F.; Dunlap, W. A.; Holditech, S. A. Oceanic Methane Hydrate Development: Reservoir Character and Extraction. In *1997 Offshore Technology Conference*, Houston, TX, 1997; 8300 pp.
(30) Wu, M.; Wang, S.; Liu, H. A study on inhibitors for the prevention of hydrate formation in gas transmission pipeline. *J. Nat. Gas Chem.* **2007**, *16*, 81−85.
(31) Carroll, J. J. *Natural Gas Hydrates: A Guide for Engineers*, 2nd Edition; Gulf Professional Publishing: Houston, TX, 2009.
(32) Englezos, P. Clathrate Hydrates. *Ind. Eng. Chem. Res.* **1993**, *32*, 1251−1274.
(33) Kvenvolden, K. A. Gas hydrates—Geological perspective and global change. *Rev. Geophys.* **1993**, *31*, 173−187.
(34) Sloan, D. E.; Koh, C. A. *Clathrate Hydrates of Natural Gases*, 3rd Edition; CRC Press/Taylor and Francis Group: Boca Raton, FL, 2008.
(35) Frostman, L. M. *Anti-agglomerant Hydrate Inhibitors for Prevention of Hydrate Plugs in Deepwater Systems*; Society of Petroleum Engineers: Richardson, TX, 2000; pp 573−579.
(36) Frostman, L. M.; Przybylinski, J. L. *Successful Applications of Anti-agglomerates Hydrate Inhibitors*; Society of Petroleum Engineers: Richardson, TX, 2001; pp 259−268.
(37) Nihous, G. C.; Kinoshita, C. K.; Masutani, S. M. A determination of the activity of water in water-alcohol mixtures using mobile order thermodynamics. *Chem. Eng. Sci.* **2009**, *64*, 2767−2771.
(38) Lu, H. L.; Matsumato, R.; Tsuji, Y.; Oda, H. Anion plays a more important role than cation in affecting gas hydrate stability in electrolyte solution? A recognition from experimental results. *Fluid Phase Equilib.* **2001**, *178*, 225−232.
(39) Freer, E. M.; Sloan, D. E. An engineering approach to kinetic inhibitor design using molecular dynamics simulations. *Ann. N.Y. Acad. Sci.* **2000**, *912*, 766−776.
(40) Lederhos, J. P.; Longs, J. P.; Sum, A.; Christiansen, R. I.; Sloan, E. D. Effective kinetic inhibitors for natural gas hydrates. *Chem. Eng. Sci.* **1996**, *51*, 1221−1229.
(41) Karaaslan, U.; Parlaktuna, M. PEO—A new hydrate inhibitor polymer. *Energy Fuels* **2002**, *16*, 1387−1391.
(42) Marsh, K. N.; Deev, A.; Wu, A. C. T.; Tran, E. Room temperature ionic liquids as replacements for conventional solvents—A review. *Korean J. Chem. Eng.* **2002**, *19*, 357−362.
(43) Plechkova, N. V.; Seddon, K. R. Applications of ionic liquids in the chemical industry. *Chem. Soc. Rev.* **2008**, *37*, 123−150.
(44) Welton, T. Room temperature ionic liquids: Solvents for synthesis and catalysis. *Chem. Rev.* **1999**, *99*, 2071−2084.
(45) Esperanca, J. M. S. S.; Lopes, J. N. C.; Tariq, M.; Luis, J.; Magee, W.; Rebelo, L. P. N. Volatility of aprotic ionic liquids—A Review. *J. Chem. Eng. Data* **2010**, *55*, 3−12.
(46) Tariq, M.; Fereire, M.; Saramago, B.; Lopes, J. N. C.; Coutinho, J. A. P.; Rebelo, L. P. N. Surface Tension of Ionic Liquids and ionic liquid solutions. *Chem. Soc. Rev.* **2012**, *41*, 829−868.
(47) Chen, Q.; Yu, Y.; Zeng, P.; Yang, W.; Liang, Q.; Peng, X.; Liu, Y.; Hu, Y. Effect of 1-butyl-3-methylimidazolium tetrafluoroborate on the formation rate of CO_2 hydrate. *J. Nat. Gas Chem.* **2008**, *17*, 264−267.
(48) Xiao, C.; Adidharma, H. Dual function inhibitors for methane hydrate. *Chem. Eng. Sci.* **2009**, *64*, 1522−1527.
(49) Xiao, C.; Wibisono, N.; Adidharma, H. Dialkylimidazolium halide ionic liquids as dual function inhibitors for methane hydrate. *Chem. Eng. Sci.* **2010**, *65*, 3080−3087.
(50) Del Villano, L.; Kelland, M. A. An investigation into the kinetic hydrate inhibitor properties of two imidazolium-based ionic liquids on Structure II gas hydrate. *Chem. Eng. Sci.* **2010**, *65*, 5366−5372.
(51) Peng, X.; Hu, Y.; Liu, Y.; Jin, C.; Lin, H. Separation of ionic liquids from dilute aqueous solutions using the method based on CO_2 hydrates. *J. Nat. Gas Chem.* **2010**, *19*, 81−85.
(52) Xiao-Sen, L.; Yi-Jun, L.; Zhi-Yong, Z.; Zhao-Yang, C.; Gang, L.; Hui-Jie, W. Equilibrium hydrate formation conditions for the mixtures of methane + ionic liquids + water. *J. Chem. Eng. Data* **2011**, *56*, 119−123.
(53) Tumba, K.; Reddy, P.; Naidoo, P.; Ramjugernath, D. Phase equilibria of methane and carbon dioxide clathrate hydrates in the presence of aqueous solutions of tributylmethylphosphonium methylsulfate ionic liquid. *J. Chem. Eng. Data* **2011**, *56*, 3620−3629.
(54) Nazari, K.; Ahmadi, A. N.; Moradi, M. R.; Sahraei, V.; Taghikhani, V.; Ghobti, C.A thermodynamic study of methane hydrate formation in the presence of [BMIM][BF_4] and [BMIM][MS] ionic liquids. In *Proceedings of the 7th International Conference on Gas Hydrates (ICGH 2011)*, Edinburgh, Scotland, U.K., July 17−21, 2011 (Paper No. 378).
(55) Kim, K.-S.; Kang, S.-P. Investigation of pyrrolidinium- and morpholinium- based ionic liquids into kinetic hydrate inhibitors on structure I methane hydrate. In *Proceedings of the 7th International Conference on Gas Hydrates (ICGH 2011)*, Edinburgh, Scotland, U.K., July 17−21, 2011 (Paper No. 593).
(56) Makino, T.; Matsumoto, Y.; Sugahara, T.; Ohgaki, K.; Masuda, H. Effect of ionic liquid on hydrate formation rate in carbon dioxide hydrates. In *Proceedings of the 7th International Conference on Gas Hydrates (ICGH 2011)*, Edinburgh, Scotland, U.K., July 17−21, 2011 (Paper No. 554).
(57) Kim, K.-S.; Kang, J. W.; Kang, S.-P. Tuning ionic liquids for hydrate inhibition. *Chem. Commun.* **2011**, *47*, 6341−6343.
(58) Kitajima, T.; Ohtsubo, N.; Hashimoto, S.; Makino, T.; Kodama, D.; Ohgaki, K. Study on prompt methane hydrate formation derived by addition of ionic liquid. *Am. Chem. Sci. J.* **2012**, *2*, 100−110.
(59) Richard, A. R.; Adidharma, H. The performance of ionic liquids and their mixtures in inhibiting methane hydrate formation. *Chem. Eng. Sci.* **2013**, *87*, 270−276.
(60) Partoon, B.; Wong, N. M. S.; Sabil, K. M.; Nasrifar, K.; Ahmad, M. R. A study on thermodynamics effect of [EMIM]-Cl and [OH-C_2MIM]-Cl on methane hydrate equilibrium line. *Fluid Phase Equilib.* **2013**, *337*, 26−31.
(61) Zare, M.; Haghtalab, A.; Ahmadi, A. N.; Nazari, K. Experiment and thermodynamic modeling of methane hydrate equilibria in the presence of aqueous imidazolium-based ionic liquid solutions using electrolyte cubic square well equation of state. *Fluid Phase Equilib.* **2013**, *341*, 61−69.
(62) Chun, L. K.; Jaafar, A. Ionic liquid as low dosage hydrate inhibitor for flow assurance in pipeline. *Asian J. Sci. Res.* **2013**, *6*, 374−380.
(63) Keshavarz, L.; Javanmardi, J.; Eslamimanesh, A.; Mohammadi, A. H. Experimental measurement and modeling of methane hydrate

dissociation conditions in the presence of aqueous solutions of ionic liquid. *Fluid Phase Equilib.* **2013**, *354*, 312−318.
(64) Ebrahim, M.; Nasrollaha, H.; Abareshia, B.; Ghotbi, C.; Taghikhania, V.; Jalilib, A. H. Investigation of Six Imidazolium-Based Ionic Liquids as Thermo-Kinetic Inhibitors for Methane Hydrate by Molecular Dynamics Simulation. Presented at the *2nd National Iranian Conference on Gas Hydrate (NICGH)*.
(65) Adidharma, H.; Xiao, C. *Dual Function Gas Hydrate Inhibitors*, U.S. Patent Application No. 20110152130 A1, June 23, 2011.
(66) Najibi, H.; Chapoy, A.; Haghigi, H.; Tohidi, B. Experimental determination and prediction of methane hydrate stability in alcohols and electrolyte solutions. *Fluid Phase Equilib.* **2009**, *275*, 127−131.
(67) Haghigi, H.; Chapoy, A.; Tohidi, B. Methane and water phase equilibria in the presence of single and mixed electrolyte solutions using the cubic-plus-association equation of state. *Oil Gas Sci. Technol. Rev.* **2009**, *64*, 141−154.
(68) Mohammadi, A. H.; Richon, D. Methane hydrate phase equilibrium in the presence of salt (NaCl, KCl, or $CaCl_2$) + ethylene glycol or salt (NaCl, KCl, or $CaCl_2$) + methanol aqueous solution: Experimental determination of dissociation condition. *J. Chem. Thermodyn.* **2009**, *41*, 1374−1377.
(69) Behar, H.; Delion, A. S.; Herri, J. M.; Sugier, A.; Thomas, M. Plugging control of production facilities by hydrates. *Ann. N.Y. Acad. Sci.* **1994**, *715*, 94−105.
(70) Verdoes, D.; Kashchiev, D.; van Rosmalen, G. M. Determination of nucleation and growth rates from induction times in seeded and unseeded precipitation of calcium carbonate. *J. Cryst. Growth* **1992**, *118*, 401−413.
(71) Mohammadi, A. H.; Richon, D. Development of predictive techniques for estimating liquid water−hydrate equilibrium of water−hydrocarbon system. *J. Chem. Thermodyn.* **2009**, *48*, 1−12.
(72) Mohammadi, A. H.; Richon, D. Thermodynamic model for predicting liquid water−hydrate equilibrium of water−hydrocarbon system. *J. Chem. Thermodyn.* **2008**, *47*, 1346−1350.
(73) Holder, G. D.; Corbin, G.; Papadopoulos, D. J. Thermodynamic and molecular properties of gas hydrates from mixtures containing methane, argon and krypton. *Ind. Eng. Chem. Fundam.* **1980**, *19*, 282−286.
(74) Peng, D. Y.; Robinson, D. B. A new two-constant equation of state. *Ind. Eng. Chem. Fundam.* **1976**, *15*, 59−64.
(75) van der Waal, J. H.; Platteeuw, J. C. Clathrate solutions. *Adv. Chem. Phys.* **1959**, *2*, 1−57.
(76) Renon, H.; Prausnitz, J. M. Liquid−liquid and vapour−liquid equilibria for binary and ternary systems with dibutyl ketone, dimethylsulfoxide, *n*-hexane and 1-hexene. *Ind. Eng. Chem. Process. Des. Dev.* **1968**, *7*, 220−225.
(77) Aznar, M. Correlation of (liquid + liquid) equilibrium of systems including ionic liquids. *Braz. J. Chem. Eng.* **2007**, *24*, 143−149 (DOI: 10.1590/S0104-66322007000100013).
(78) Maddox, R. N.; Moshfeghian, M.; Lopez, E.; Tu, C. H.; Shariat, A.; Flynn, J. Predicting hydrate temperature at high inhibitor concentration. In *Proceedings of the Laurance Reid Gas Conditioning Conference*, Norman, OK, 1991; pp 273−294.
(79) Pitzer, K. H.; Mayogra, G. Thermodynamics of electrolytes. II. Activity and osmotic coefficients for strong electrolytes with one or both ions univalent. *J. Phys. Chem.* **1973**, *77*, 2300−2308.
(80) Liao, Z.; Guo, X.; Zhao, Y.; Wang, Y.; Sun, Q.; Liu, A.; Sun, C.; Chen, G. Experimental and Modeling Study on Phase Equilibria of Semiclathrate Hydrates of Tetra-*n*-butyl ammonium bromide + CH_4, CO_2, N_2, or Gas Mixtures. *Ind. Eng. Chem. Res.* **2013**, *52*, 18440−18446.
(81) Jiang, H.; Adidharma, H. Modeling of Hydrate Dissociation Conditions for Alkanes in the Presence of Single and Mixed Electrolyte Solutions Using Ion-Based Statistical Associating Fluid Theory. *Ind. Eng. Chem. Res.* **2012**, *51*, 5818−5825.
(82) Jiang, H.; Adidharma, H. Thermodynamic modeling of aqueous ionic liquid solutions and prediction of methane hydrate dissociation conditions in the presence of ionic liquids. *Chem. Eng. Sci.* **2013**, *102*, 24−31.
(83) Li, S.; Fan, S.; Wang, J.; Lang, X.; Wang, Y. Semicathrate hydrate phase equilibrium for CO_2 in the presence of tetra-*n*-butyl ammonium halide (bromide, chloride, or fluoride). *J. Chem. Eng. Data* **2010**, *55*, 3212−3215.
(84) Makino, T.; Yamamato, T.; Nagata, K.; Sakamoto, H.; Hashimoto, S.; Sugahara, T.; Ohgaki, K. Thermodynamic stabilities of tetra-*n*-butyl ammonium chloride + H_2, N_2, CH_4, CO_2 or C_2H_6 semiclathrate hydrate systems. *J. Chem. Eng. Data* **2010**, *55*, 839−841.
(85) Mayoufi, N.; Dalmazzone, D.; Furst, W.; Delahaye, A.; Fournaison, L. CO_2 enclathration in hydrates of peralkyl-(ammonium/phosphonium) salts: Stability conditions and dissociation enthalpies. *J. Chem. Eng. Data* **2010**, *55*, 1271−1275.
(86) Deschamps, J.; Dalmazzone, D. Hydrogen storage in semi clathrate hydrates of tetrabutyl ammonium chloride and tetrabutylphosphonium bromide. *J. Chem. Eng. Data* **2010**, *55*, 3395−3399.
(87) Lee, S.; Lee, Y.; Park, S.; Seo, Y. Phase equilibria of semiclathrate hydrate for nitrogen in the presence of tetra-*n*-butylammonium bromide and fluoride. *J. Chem. Eng. Data* **2010**, *55*, 5883−5886.
(88) Mohammadi, A. H.; Richon, D. Phase equilibria of semi clathrate hydrates of tetra-*n*-butylammonium bromide + methane. *J. Chem. Eng. Data* **2010**, *55*, 982−984.
(89) Petkovic, M.; Seddon, K. R.; Rebelo, L. P. N.; Pereira, C. S. Ionic liquids: A pathway to environmental acceptability. *Chem. Soc. Rev.* **2011**, *40*, 1383−1403.